

MODIS Land Bands for Ocean Remote Sensing Applications

Bryan A. Franz^{1,2}, P. Jeremy Werdell^{1,3}, Gerhard Meister^{1,4}, Ewa J. Kwiatkowska^{1,2},
Sean W. Bailey^{1,4}, Ziauddin Ahmad^{1,5}, and Charles R. McClain¹

¹NASA Goddard Space Flight Center, Greenbelt, Maryland, USA

²Science Applications International Corporation, San Diego, California, USA

³Science Systems and Applications, Inc., Lanham, Maryland, USA

⁴Futuretech Corporation, Greenbelt, Maryland, USA

⁵Science and Data Systems, Inc., Silver Spring, Maryland, USA

INTRODUCTION

The Ocean Biology Processing Group (OBPG) at NASA's Goddard Space Flight Center provides the global processing and distribution of ocean color products from MODIS (Esaias et al. 1998), SeaWiFS (McClain et al. 1998), and other ocean color capable sensors. The fundamental measurement in ocean color remote sensing is the spectral distribution of radiance upwelling from the ocean, or water-leaving radiance, as this information can be used to derive various geophysical parameters such as chlorophyll concentration (Clark et al. 1970). However, space borne ocean color sensors actually observe the total radiance exiting the top of the atmosphere (TOA), of which at least 90% is scattered Sun light from aerosols and air molecules that never penetrated the ocean surface. The retrieval of water-leaving radiance from observed TOA radiance requires a process generally referred to as atmospheric correction. The OBPG developed the Multi-Sensor Level-1 to Level-2 code (MSL12, Franz 2006) to standardize the atmospheric correction and production of ocean color products from various space borne sensors (e.g., Franz et al. 2005).

The MODIS instrument was designed with 36 spectral channels to support observation of clouds and land as well as oceans. The traditional channels used for ocean color observation are the 9 bands in the visible to near infrared (NIR) spectral regime from 412-869 nm, which have a spatial resolution of approximately 1 km at nadir. These ocean bands were designed with high sensitivity over the range of reflectance typical of open ocean observations with maritime atmospheric conditions. Over highly turbid coastal and inland waters it is possible for this dynamic range to be exceeded, such that the bands saturate and the true signal is unknown. Other bands on MODIS were specifically designed for land and cloud observations, with both increased spatial resolution and reduced sensitivity over a broader dynamic range. These land/cloud bands overlap the spectral range of the ocean bands and extend into the short-wave infrared (SWIR), from 469 to 2130 nm, with a spatial resolution of 250 to 500-meters at nadir. A number of investigators have looked to exploit this additional information for ocean application. For example, Gao et al. (2000) developed a generalized processing code that was able to utilize the full spectral range of MODIS, and Li et al. (2003) proposed a method to use the expanded dynamic range of the land/cloud channels for the detection of suspended sediments and ocean bottom reflectance. Arnone et al. (2002) developed a technique for enhancing the resolution of inherent optical property retrievals (water absorption and backscatter) in coastal areas using the 250-meter channel at 645 nm, while other investigators have used the higher resolution bands to assess estuarine water quality (Hu et al. 2004) or identify harmful algal blooms (Kahru et al. 2004). Recently, Wang & Shi (2005) demonstrated an approach for utilizing the SWIR bands to improve the performance of the Gordon & Wang (1994) atmospheric correction algorithm over turbid or highly productive waters typically found in coastal environments.

The OBPG has now enhanced MSL12 to support the 250 and 500-meter bands of MODIS (herein referred to as the high resolution or HIRES bands). The extended band suite is shown in Table 1 (for completeness, the thermal bands used by MSL12 for sea surface temperatures are shown in Table 2). This effort began with characterization of the radiometric response of the HIRES bands in a manner consistent with that done for the standard ocean bands. The appropriate software and tables were then developed to facilitate the atmospheric correction and retrieval of oceanic optical properties at the additional wavelengths. A mechanism was also developed for accessing the increased spatial resolution, and options were added for utilizing the SWIR information for atmospheric correction. The OBPG is distributing these enhanced capabilities through the SeaWiFS Data Analysis System (SeaDAS, Baith et al. 2001) software package. In the sections that follow, we describe our approach to incorporation of the HIRES bands into the ocean processing code and demonstrate application of these new capabilities to the coastal and inland waters of the Chesapeake Bay region. The goal of this effort is to provide a tool to the research community for evaluating and developing applications of the HIRES bands to ocean remote sensing.

Table 1: Extended MODIS Band Suite for Oceans

Band Number	Wavelength (nm)	Band Width (nm)	Spatial Resolution (m)	SNR at L_{typ}	L_{typ} $mW\ cm^{-2}\ \mu m^{-1}\ sr^{-1}$	L_{max} $mW\ cm^{-2}\ \mu m^{-1}\ sr^{-1}$	Notes
8	412	15	1000	1773	7.84	26.9	1
9	443	10	1000	2253	6.99	19.0	1
3	469	20	500	556	6.52	59.1	
10	488	10	1000	2270	5.38	14.0	1
11	531	10	1000	2183	3.87	11.1	1
12	551	10	1000	2200	3.50	8.8	1
4	555	20	500	349	3.28	53.2	
1	645	50	250	140	1.65	51.2	3
13	667	10	1000	1962	1.47	4.2	1
14	678	10	1000	2175	1.38	4.2	1
15	748	10	1000	1371	0.889	3.5	1
2	859	35	250	103	0.481	24.0	
16	869	15	1000	1112	0.460	2.5	1
5	1240	20	500	25	0.089	12.3	
6	1640	35	500	19	0.028	4.9	2
7	2130	50	500	12	0.008	1.7	

¹ Standard bands for ocean color, ² 1640 channel not functional on MODIS/Aqua, ³ Never saturated

Table 2: Thermal Bands for SST

Band Number	Wavelength (μm)	Spatial Resolution (m)
22	3.9	1000
23	4.0	1000
31	11	1000
32	12	1000

CALIBRATION AND CHARACTERIZATION

The interpretation of radiometric observations from any multi-spectral sensor must begin with a full understanding of the instrument characteristics. The MODIS Characterization Support Team (MCST) is responsible for the instrument calibration and characterization of MODIS (e.g., Xiong et al. 2003). MCST incorporates the pre-launch knowledge of radiometric response to known sources and varying temperatures, as well as temporal change derived from on-orbit calibrations to the moon, sun, and internal sources into a look-up table (LUT) that defines the instrument calibration. The MODIS instrument response is also sensitive to the polarization properties of the light scattered from the ocean and atmosphere. The polarization sensitivity of the instrument was measured by the manufacturer prior to launch, and the OBPG developed the polarization LUTs for the standard ocean bands (Meister et al. 2005) based on an analysis of these pre-launch measurements. This analysis was extended to include the HIRES bands. The MSL12 code incorporates a polarization correction for MODIS based on Gordon et al. (1997). Figure 1 shows the polarization correction factor over a range of polarization rotation angles for all visible and NIR wavelengths of Table 1 (from Meister 2006).

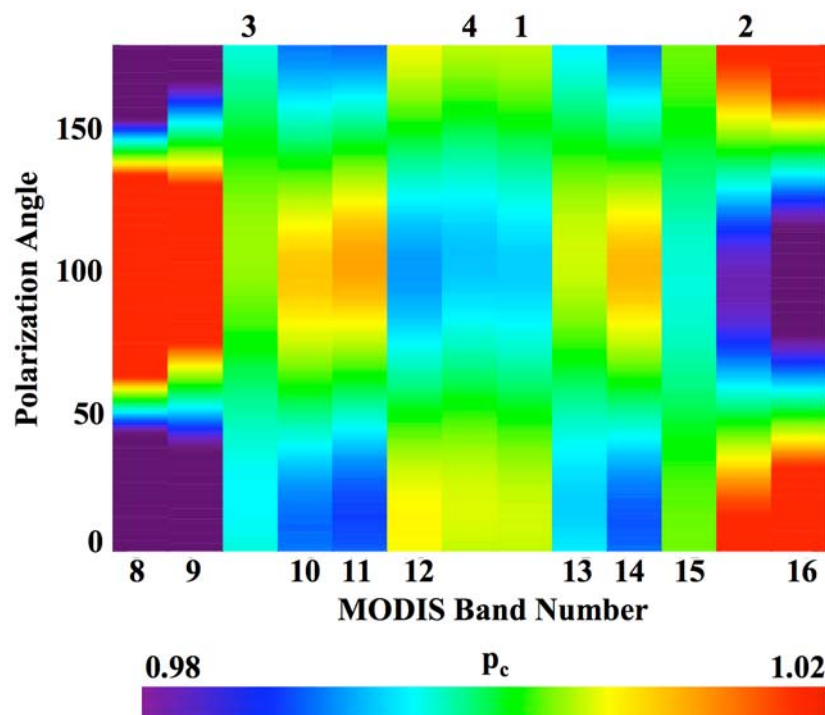


Figure 1: Polarization correction (p_c) for MODIS/Aqua for a sensor view angle of 45 degrees. The spectral bands are presented in wavelength order, with the MODIS band number given on the bottom for the standard ocean bands and on top for the HIRES bands (from Meister 2006).

Finally, the OBPG performed a vicarious calibration to ground truth (Werdell et al. 2006). This calibration adjusts for any residual instrument calibration error as well as any systematic bias in the atmospheric correction algorithm such that the system, on average, reproduces a set of *in situ* observations of water-leaving radiance. Using a series of match-ups between MODIS observations and the Marine Optical Buoy (MOBY, Mueller et al. 2003), where the hyper-spectral MOBY

observations were convolved with the full relative spectral response of each MODIS band, the OBPB derived the set of multiplicative gain factors for MODIS/Aqua shown in Table 3. Since water is a near perfect absorber in the SWIR spectral regime, the adjustment of the SWIR bands is just that required to yield zero water-leaving radiance in the clear waters surrounding MOBY.

Table 3: Vicarious Calibration Gains for MODIS/Aqua

Band	412	443	469	488	531	551	555	645
Gain	0.9710	0.9848	1.002	0.9795	0.9870	0.9850	0.9842	1.0049
Band	667	678	748	859	869	1240	1640	2130
Gain	0.9797	0.9776	0.9855	1.030	1.000	1.055	-	1.115

Table 1 also presents the signal-to-noise ratio (SNR) at a typical TOA radiance (L_{typ}) and the maximum observable radiance in each channel (L_{max}) of the extended band suite. The L_{typ} was derived by averaging cloud-free pixels over mesotrophic waters for a range of viewing and solar geometries and the L_{max} is the peak radiance preceding saturation, where both were obtained by analysis of a series of scenes distributed over the duration of the MODIS/Aqua mission. Results for MODIS/Terra should be similar. The SNR was determined at L_{typ} based on relationships derived on-orbit and reported by Xie et al. (2003). Comparing, for example, the 469 and 488 nm bands, Table 1 shows that the 469 nm band can reach a much higher radiance than the spectrally adjacent ocean band. This expanded dynamic range, however, is spread over the same 12-bit digital storage of the instrument, so a digital count in the 469-nm band represents a larger step in radiance than that of the equivalent ocean band (Hu et al., 2004). In addition, the enhanced resolution of the HIRES bands is obtained at the cost of shorter integration times, which contributes to a reduced signal-to-noise ratio. The higher noise levels may result in erroneous, small-spatial-scale variability in ocean products derived using these bands.

Furthermore, images of the observed radiances or derived geophysical products from MODIS may show systematic artifacts that appear as stripes running perpendicular to the orbit track. At 1 km resolution, such striping occurs in patterns with a 10-line repeat cycle. This effect is due to imperfect relative corrections between the 10 along-track detectors associated with each 1-km band. For the 500 and 250-meter bands, 20 and 40 detectors are distributed along-track to provide the higher along-track resolution. As such, cross-track striping artifacts at 20 and 40 line intervals can occur for the 500 and 250-meter bands, respectively. This problem is exacerbated by the higher digitization error of these bands, as a single count difference between detectors can sometimes be a significant fraction of the water-leaving radiance that we wish to retrieve. In addition, within each physical scan of MODIS, the 500-meter detector sets are sampled at double the rate of the 1-km detectors, and the 250-meter detectors are sampled at four times the rate. This temporal sub-sampling is what provides the higher cross-track pixel resolution. Slight variation in the temporal sub-sampling rate or imperfect reset of the sampling registers can give rise to vertical (along-track) striping in the higher resolution bands. Corrections have been applied for these effects, but the corrections will never be perfect. Both along-track and cross-track striping artifacts may occur in image products derived with the HIRES bands.

DATA PROCESSING CAPABILITIES

MSL12 supports the processing of TOA radiances from a variety of sensors to Level-2 geophysical products. Two of the sensors supported are MODIS on Aqua and MODIS on Terra. The MODIS Level-1B product format (Isaacman et al. 2003) provides the calibrated TOA radiances in three separate files corresponding to the three distinct spatial resolutions of 250, 500, and 1000-meters with filename identifiers QKM, HKM, and 1KM, respectively. The spectral bands associated with each file are provided in Table 4. Note that the HKM file also includes the two 250-meter bands. The radiances from the 250-meter bands are averaged to 500-meter spatial resolution and written to special "aggregated" fields in the HKM file. Similarly, the radiances from the 250 and 500-meter bands are averaged to 1000-meter resolution and stored in the 1KM file. A standard 1KM Level-1B product therefore includes the full spectral band suite shown in Table 1 (as well as other bands), but the nadir resolution has been reduced to 1 km for all bands.

Table 4: Relevant Spectral Bands as Distributed in Each Level-1B File Type

QKM	HKM	1KM
645 nm	469 nm	412 nm
859 nm	555 nm	443 nm
	645 nm ¹	469 nm ³
	859 nm ¹	488 nm
	1240 nm	531 nm
	1640 nm	551 nm
	2130 nm	555 nm ³
		645 nm ²
		667 nm
		678 nm
		748 nm
		859 nm ²
		869 nm
		1240 nm ³
		1640 nm ³
		2130 nm ³
		3.9 um
		4.0 um
		11 um
		12 um

¹ 250-meter observations aggregated to 500-meter resolution,

² 250-meter observations aggregated to 1000-meter resolution,

³ 500-meter observations aggregated to 1000-meter resolution.

MSL12 has been enhanced to support processing at 250 and 500-meter resolution, in addition to the standard 1 km processing. When processing at 250-meters, the radiances of the 500-meter and 1000-meter bands are bi-linearly interpolated to 250-meter resolution such that the full band set is co-registered. When processing at lower resolutions, the radiances of the higher resolution bands will be read from the appropriate aggregated field of the lower resolution file. The geolocation information

provided for MODIS defines the centers of the 1 km pixels, so MSL12 will perform appropriate interpolations when processing at higher resolutions. All interpolations follow the methodology outlined by Gumley et al. (2003). The longitudes, latitudes, and radiant-path geometries (solar and sensor view zenith and azimuth) are similarly interpolated, as are the radiances when going from lower to higher spatial resolutions. The homogenization of the spatial resolution ensures that all derived-product algorithms included in MSL12 (e.g., various chlorophyll algorithms, diffuse attenuation, and even sea surface temperature) can be operated at any of the three resolutions, regardless of the specific wavelengths required to generate the product. It must be recognized, however, that only the 645 and 859 nm channels are truly observed at 250-meter resolution, so only derived products that depend exclusively on those two channels can be considered true 250-meter products.

The use of consistent interpolation or aggregation for all radiances, geolocation, and path geometries also ensures that subsequent computations to derive the atmospheric contributions (e.g, Rayleigh and aerosol scattering terms) are appropriate to the observed radiances. Following the work of Gordon & Wang (1994), the OBPG developed the Rayleigh, aerosol, and diffuse transmittance tables and band-pass specific quantities (e.g., band-averaged solar irradiances) required to operate the atmospheric correction on the additional spectral channels and derive the water-leaving radiances in a consistent manner across the extended band suite.

The additional spectral channels in the SWIR provide an opportunity to explore a variety of new atmospheric correction options that may be of particular value in highly reflective, turbid waters. The standard aerosol correction algorithm used by the OBPG (Gordon & Wang 1994) for global MODIS ocean processing makes use of the near infrared (NIR) bands at 748 and 869 nm to determine aerosol type and concentration. The method requires *a priori* knowledge of the water-leaving radiance in these longer wavelengths to separate the aerosol and water contributions to the total radiance. The OBPG employs an iteration scheme (Stumpf et al. 2003) to model and predict the water-leaving radiances in the NIR from retrieved water-leaving radiances in the visible, but the modeling approach is based on empirical relationships that may not be valid in all waters. In contrast, water is so strongly absorbing in the SWIR spectral regime that even highly reflective turbid waters appear black. Following the recent work by Wang & Shi (2005), wherein the SWIR bands at 1240 and 1640 were used to determine aerosol type and concentration, optional aerosol correction methods were developed for MSL12 to allow the determination of aerosol concentration and/or aerosol type using any combination of NIR and SWIR bands. As with standard Gordon & Wang, this information can then be extrapolated to the visible wavelengths via aerosol models. It should be noted, however, that the signal-to-noise in the SWIR bands (Table 1) is quite low, and this may be a limiting factor in any advantage gained by using the SWIR, especially where the aerosol signal is low.

Wang and Shi (2006) also proposed the use of the SWIR band at 1640 nm for cloud masking. The standard cloud masking approach is based on a surface + aerosol reflectance threshold in excess of 2.7% in the 869 nm NIR channel. Wang and Shi argued that this threshold may be exceeded by reflectivity of the water body alone, for highly reflective waters, even for clear atmospheric conditions. Use of the SWIR for cloud masking reduces the likelihood of such misclassification. Since, MODIS on Aqua does not have a working 1640 nm channel, MSL12 was modified to use the 2130 nm channel and a threshold of 1.8% for cloud detection.

As previously stated, the purpose of providing access to the HIRES bands within MSL12 is to encourage and support the development of new algorithms or applications by the research community.

At present, the additional spectral bands in the visible can be processed to water-leaving radiance or remote sensing reflectance. For the extended band set, the default product suite (Table 5) is just the standard MODIS ocean product suite with water-leaving radiances for some HIRES bands included. In addition, J. O'Reilly (personal communication) has provided a new chlorophyll algorithm based on the two 500-meter bands at 469 and 555 nm (OC2, O'Reilly et al. 2000). Unlike the standard MODIS chlorophyll algorithm (OC3; O'Reilly et al. 2000) that relies on the 1000-meter channels at 443, 488, and 551 nm, the OC2 product can provide true 500-meter chlorophyll-a retrievals. Similarly, the nLw_645 product can provide true 250-meter resolution imagery of the water-leaving radiance at 645 nm. It is expected that this product, perhaps in combination with the water-leaving radiance of the 859-nm channel, may prove useful as a high-resolution proxy for turbidity that can then be related to concentrations of suspended matter or other scattering sources (e.g., Li et al. 2003, Miller & McKee 2004, Kahru et al. 2004). In addition, there are product algorithms already available in MSL12 that can make use of the increased spectral density. For example, the 469 and 555 nm channels will be included within the optimization of the GSM01 bio-optical model (Maritorena et al. 2002).

Table 5: Default Product Suite for Extended MODIS Ocean Bands

Product	Description
chlor_a	chlorophyll-a based on OC3 algorithm
K_490	diffuse attenuation at 490 nm
nLw_412	normalized water-leaving radiance at 412 nm
nLw_443	normalized water-leaving radiance at 443 nm
nLw_469	normalized water-leaving radiance at 469 nm
nLw_488	normalized water-leaving radiance at 488 nm
nLw_531	normalized water-leaving radiance at 531 nm
nLw_551	normalized water-leaving radiance at 551 nm
nLw_555	normalized water-leaving radiance at 555 nm
nLw_645	normalized water-leaving radiance at 645 nm
nLw_667	normalized water-leaving radiance at 667 nm
nLw_678	normalized water-leaving radiance at 678 nm
sst	sea surface temperature from 11-12 μm channels
tau_869	aerosol optical thickness at 869 nm
angstrom_531	aerosol model Angstrom exponent (531 to 869 nm)
eps_78	ratio of aerosol reflectance in model selection bands

EVALUATION OF RESULTS

To demonstrate and evaluate some of the enhanced capabilities described above, a series of MODIS/Aqua scenes for the Chesapeake Bay was processed to derive water-leaving radiances, chlorophyll concentration, and other geophysical parameters. The processing was performed using both the standard NIR atmospheric correction based on Gordon & Wang (1994) and Stumpf (2003) (herein referred to as GWNIR) and a modified Gordon & Wang correction using the SWIR bands at 1240 and 2130 nm to determine the aerosol properties (GWSWIR).

Figure 2 shows an example of this analysis for a scene from the 28th of April 2003. Panel 2a shows a quasi-true-color image derived by combining the 645, 555, and 469 nm channels, while 2b is the OC3 chlorophyll product computed from water-leaving radiance retrieved using the standard GWNIR atmospheric correction. Figure 2d shows the same OC3 chlorophyll product, but the water-leaving radiances were retrieved using the alternate GWSWIR atmospheric correction. Comparing 2b and 2d, the results show a significant reduction in the high chlorophylls when using GWSWIR. Those high chlorophylls in Figure 2b are often in locations that can be expected to have a high concentration of suspended matter (i.e., shorelines and rivers), where the standard atmospheric correction tends to underestimate the scattering contributions from the water in the NIR and attribute the excess radiance to aerosols. This overestimation of aerosols and associated misidentification of aerosol type results in underestimation of the water leaving radiances in the visible bands and skews the spectral distribution toward the green. In contrast, the GWSWIR correction appears to produce a more uniform distribution of chlorophyll for this scene when using the same chlorophyll algorithm. Figure 2c shows the chlorophyll retrieved using the GWSWIR correction and the OC2 chlorophyll algorithm. Comparison between 2c and 2d indicates that the 500-meter bands at 469 and 555 nm have sufficient fidelity to produce meaningful chlorophyll concentrations.

For a demonstration of the enhanced resolution capabilities, a MODIS/Aqua scene of the Chesapeake Bay from April 5th 2004 was processed at 250-meter resolution. In the quasi-true-color image of Figure 3, patterns in the water can be qualitatively associated with river plumes carrying sediments and dissolved organic matter into the Bay. For the same region, Figure 4 shows the retrieved water-leaving radiance for the 250-meter band at 645 nm, where the fine structure of the river plumes is more discernable and quantifiable.

For a more quantitative analysis, the Bay was stratified into upper, middle, and lower regions as defined in Magnuson (2004). Monthly means from all available, relatively cloud free scenes were generated for each region (approximately 30 scenes per year), and the time-series was compared to contemporaneous *in situ* measurements collected by the Chesapeake Bay Program (1993) and Harding et al. (2003). This analysis is presented as a time-series in Figure 5. Each panel shows the monthly mean *in situ* data in black, with error bars indicating one standard deviation about the mean. The MODIS/Aqua retrievals are overlain in red symbols and lines. For the first plot of each regional panel, the satellite data was processed with standard GWNIR atmospheric correction and the chlorophyll was derived with the OC3 algorithm, while the second panel shows the same OC3 chlorophyll based on radiances retrieved via GWSWIR. Relative to the standard algorithm, the GWSWIR correction removes a significant bias between the satellite retrieved chlorophyll and field data and improves agreement over most months of the MODIS/Aqua mission. This is further illustrated in Figure 6, where the data from all months have been combined to form a set of frequency distributions. As before, the black lines are the *in situ* measurements and the red lines are retrievals from MODIS/Aqua using the OC3 chlorophyll algorithm. For the complex and sediment laden waters of the upper and middle bay, the histograms show that the GWSWIR correction significantly improves agreement between MODIS retrievals and *in situ* measurements. Even in the more oceanic waters of the lower Bay, where the mode of the distributions already showed good agreement with *in situ* for either correction method, the GWNIR approach resulted in an elevated median relative to the *in situ* distribution that was substantially reduced by application of the GWSWIR correction. This improvement is summarized by median percent difference (defined as MODIS minus *in situ* over *in situ*) in Table 6. Here it can be seen that the differences over the full time-series were reduced from a worst case of 115% in the upper Bay region to less than 17% for all regions. Furthermore, the SWIR-

based approach results in substantial improvements in the MODIS to *in situ* agreement for every season and all regions.

Table 6: Median Percent Difference Between MODIS/Aqua and In Situ Chlorophyll Measurements for Chesapeake Bay by Region and Season

Region	Method	All	Spring	Summer	Fall	Winter
Upper	GWNIR	115.3	141.5	104.7	185.8	151.2
	GWSWIR	13.3	25.2	20.5	48.6	35.8
Middle	GWNIR	94.9	87.7	122.2	113.9	148.4
	GWSWIR	15.1	-5.6	19.9	31.3	62.2
Lower	GWNIR	71.1	110.8	71.4	43.2	123.0
	GWSWIR	16.9	4.0	-4.6	13.5	72.0

CONCLUSION

The OBPB has enhanced the standard MODIS ocean color processing capabilities to utilize some additional bands originally designed for land and cloud applications. It was shown that these bands could be used to develop new ocean products at spatial resolutions as high as 250 meters, or four times the resolution of standard MODIS ocean products. Furthermore, the expanded spectral range extends into the SWIR, allowing for the operation of an alternative atmospheric correction algorithm. This SWIR-based correction was shown to significantly improve agreement between MODIS and *in situ* chlorophyll measurements in the complex and highly reflective waters of the Chesapeake Bay and would likely perform well in other coastal and inland waters where the standard atmospheric correction approach suffers. We have incorporated these new capabilities into the MSL12 processing code, which is freely distributed through SeaDAS, thereby providing the research community with an opportunity to further evaluate the alternative algorithms and perhaps develop new ocean applications using the extended spectral band suite. We caution, however, that the HIRES bands have significantly lower sensitivity relative to the ocean bands, such that elevated noise levels may limit the value gained by enhanced resolution or increased spectral information.

REFERENCES

Arnone, R.A, Z.P. Lee, P. Martinolich, B. Casey, and S.D. Ladner (2002). Characterizing the optical properties of coastal waters by coupling 1 km and 250 m channels on MODIS – Terra, *Proc. Ocean Optics XVI*, Santa Fe, New Mexico, 18-22 November.

Baith, K., R. Lindsay, G. Fu, and C.R. McClain (2001). Data analysis system developed for ocean color satellite sensors. *EOS Transactions AGU*, 82, 202. <http://oceancolor.gsfc.nasa.gov/seadas/>.

Chesapeake Bay Program (1993). Guide to using Chesapeake Bay Program Water Quality Monitoring Data. CBP/TRS 78/92, Chesapeake Bay Program, Annapolis, Maryland, 127 pp.

Clark, G.L., G.C. Ewing, and C.J. Lorenzen (1970). Spectra of backscattered light from the sea obtained from aircraft as a measure of chlorophyll concentration. *Science*, 167, 1119-1121.

Eplee, Jr., R.E. and 7 co-authors (2001). Calibration of SeaWiFS. II. Vicarious techniques. *Applied Optics*, 40, 6701-6718.

Esaias, W.E. and 12 co-authors (1998). An overview of MODIS capabilities for ocean science observations. *IEEE Transactions on Geoscience and Remote Sensing*, 36, 1250-1265.

Franz, B.A. and 9 co-authors (2005). The continuity of ocean color measurements from SeaWiFS to MODIS. In J.J. Butler (Ed.), *Proceedings SPIE*, 5882, doi:10.1117/12.620069.

Franz, B.A. (2006). MSL12: The Multi-Sensor Level-1 to Level-2 Code, Ocean Color Web, URL <http://oceancolor.gsfc.nasa.gov/DOCS/MSL12/>.

Gao, B.-C., M.J. Montes, Z. Ahmad, and C. O. Davis (2000). Atmospheric correction algorithm for hyperspectral remote sensing of ocean color from space, *Applied Optics*, 39, 887-896.

Gordon, H.R., and M. Wang (1994). Retrieval of water-leaving radiance and aerosol optical-thickness over the oceans with SeaWiFS – a preliminary algorithm. *Applied Optics*, 33, 443-452.

Gordon, H.R., T. Du, T. Zhang (1997). Atmospheric Correction of Ocean Color Sensors: Analysis of the Effects of Residual Instrument Polarization Sensitivity, *Applied Optics*, 36, 6938-6948.

Gumley, L., J. Desclotres, J. Schmaltz (2003). Creating Reprojected True-Color Images, URL http://rapidfire.sci.gsfc.nasa.gov/faq/MODIS_True_Color.pdf, 14 November 2003, pp 12-13.

Harding, L.W. and A. Magnuson (2003). Bio-Optical and Remote Sensing Observations in Chesapeake Bay, in SIMBIOS Project 2003 Annual Reports, NASA/TM-2003-212251, pp 84-97.

Hu, C., Z. Chen, T.D. Clayton, P. Swarzenski, J.C. Brock, and F.E. Müller-Karger (2004). Assessment of estuarine water-quality indicators using MODIS medium-resolution bands: Initial results from Tampa Bay, FL, *Remote Sensing of Environment*, 93, 423-441.

Isaacman, A., G. Toller, B. Guenther, W.L. Barnes, and X. Xiong (2003). MODIS Level-1B Calibration and Data Products, *Proc. SPIE Earth Observing Systems VIII*, 5151, 552-562.

Kahru, M., B.G. Mitchell, A. Diaz, M. Miura (2004). MODIS Detects Devastating Algal Bloom in Paracas Bay, Peru, *EOS Trans. AGU*, 85 (45), 465-472.

Li, R.-R., Y.J. Kaufman, B.-C. Gao, and C.O. Davis (2003). Remote Sensing of Suspended Sediments and Shallow Coastal Waters, *IEEE Trans. on Geoscience and Remote Sensing*, Vol. 41, No. 3 pp. 559.

Magnuson, A., L.W. Harding Jr., M.E. Mallonee and J.E. Adolf (2004). Bio-optical model for Chesapeake Bay and the middle Atlantic bight. *Estuar. Coast. Shelf Sci.* 61:403-424 .

Maritorena S., D.A. Siegel and A. Peterson (2002). Optimization of a Semi-Analytical Ocean Color Model for Global Scale Applications. *Applied Optics*, 41(15): 2705-2714.

McClain, C.R., M.L. Cleave, G.C. Feldman, et al. (1998). Science quality SeaWiFS data for global biosphere research, *Sea Technol.* 39: (9) 10-16.

Meister, G., E.J. Kwiatkowska, B.A. Franz, F.S. Patt, G.C. Feldman, C.R. McClain (2005). Moderate-Resolution Imaging Spectroradiometer ocean color polarization correction. *Applied Optics*, 44(26): 5524-5535

Meister, G., E.J. Kwiatkowska, and C.R. McClain (2006). Analysis of image striping due to polarization correction artifacts in remotely sensed ocean scenes. *Proc. SPIE Earth Observing Systems XI*, 6296.

Miller, R.L. and B.A. McKee (2004). Using MODIS Terra 250 m imagery to map concentrations of total suspended matter in coastal waters, *Remote Sensing of Environment*, 93, 259-266.

Mueller, J.L. and 26 co-authors (2003). *Ocean Optics Protocols for Satellite Ocean Color Sensor Validation, Vol. 6, Rev. 4: Special Topics in Ocean Optics Protocols and Appendices*. NASA Tech. Memo. 211621, NASA Goddard Space Flight Center, Greenbelt, Maryland, pp 148.

O'Reilly, J.E. and 24 co-authors (2000). *SeaWiFS Postlaunch Calibration and Validation Analyses, Part 3*. NASA Tech. Memo. 206892, Vol. 11, NASA Goddard Space Flight Center, Greenbelt, Maryland, pp 24.

Stumpf, R.P., R.A. Arnone, R.W. Gould, P.M. Martinolich, V. Ransibrahmanakul (2003). A Partially Coupled Ocean-Atmosphere Model for Retrieval of Water-Leaving Radiance from SeaWiFS in Coastal Waters, NASA/TM-2003-206892, Vol. 22 NASA Goddard Space Flight Center, Greenbelt, Maryland, pp. 51-59.

Wang, M. and W. Shi (2005). Estimation of ocean contribution at the MODIS near-infrared wavelengths along the east coast of the U.S.: Two case studies, *Geophys. Res. Lett.*, 32, L13606, doi:10.1029/2005GL022917.

Wang, M. and W. Shi (2006). Cloud Masking for Ocean Color Data Processing in the Coastal Regions, *IEEE Trans. Geosci. Remote Sensing*, accepted April 6, 2006.

Werdell, P.J., B.A. Franz, S.W. Bailey, and C.R. McClain (2006). Recent Advances in the Operational Vicarious Calibration of Visible and Near-infrared Ocean Color Radiometry, *Proc. Ocean Optics XVIII*, Montreal, Canada, 9-13 October 2006.

Xie, X., J. Sun, X. Xiong (2003). Terra and Aqua signal to noise ratio (SNR), *MCST Internal Memorandum*, M1079, 31 December.

Xiong, X., K. Chiang, J. Esposito, B. Guether, W. Barnes (2003). MODIS on-orbit calibration and characterization, *Metrologia*, 40, S89-S93.

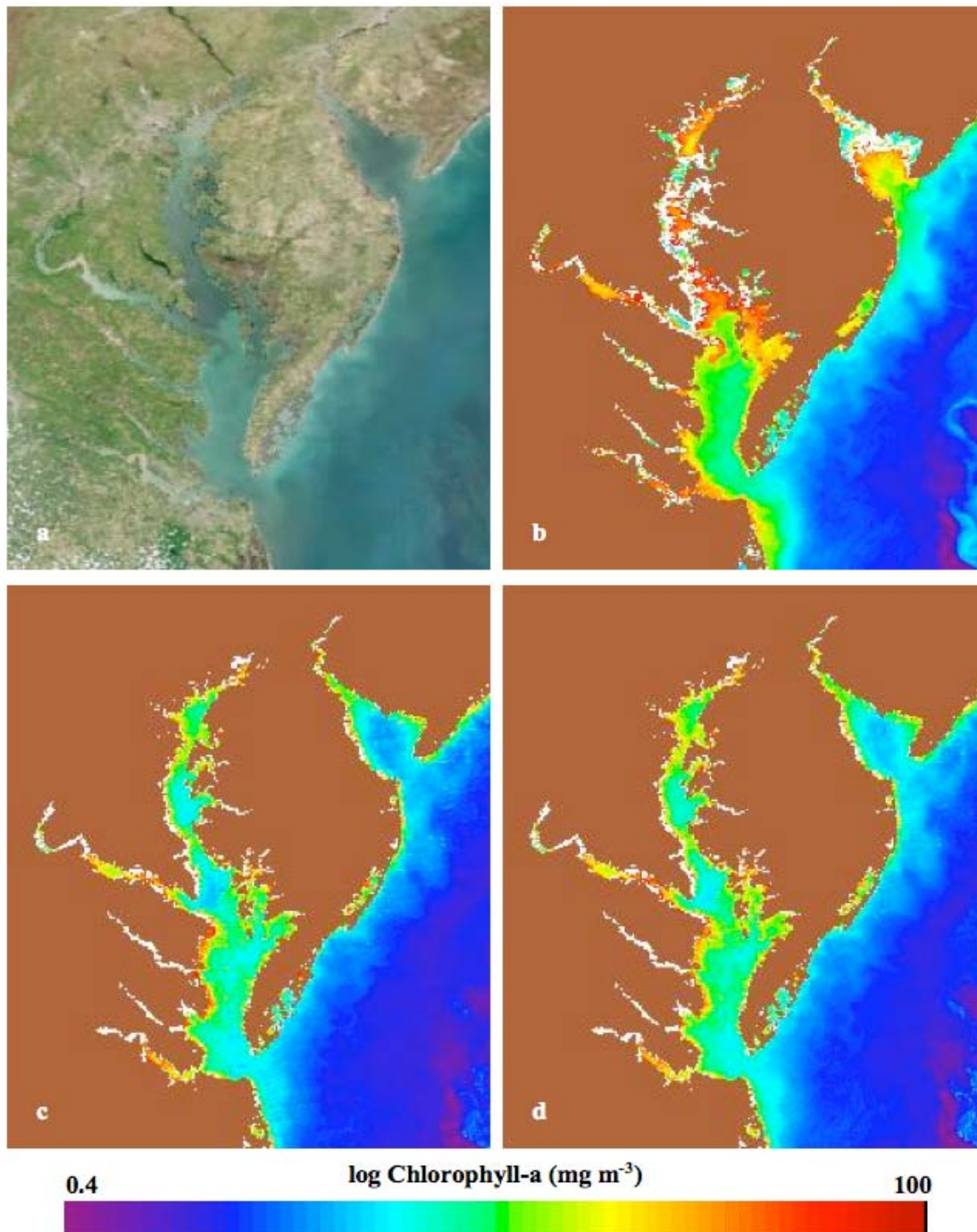


Figure 2: Sample images showing (a) a true color view of the Chesapeake Bay on 28 April 2003 derived from surface reflectance in MODIS bands at 469, 555, and 645 nm; (b) chlorophyll-a derived from the OC3 algorithm using the standard NIR-based aerosol correction; (c) & (d) chlorophyll-a derived from the OC2 & OC3 algorithms, respectively, using the SWIR-based approach for aerosol correction.



Figure 3: Quasi-true-color image of Chesapeake Bay on 5 April 2004, derived from MODIS/Aqua bands at 645, 555, and 469 nm. Data was processed at 250-meter resolution and mapped to 255-meter resolution (0.003-deg, equirectangular projection).

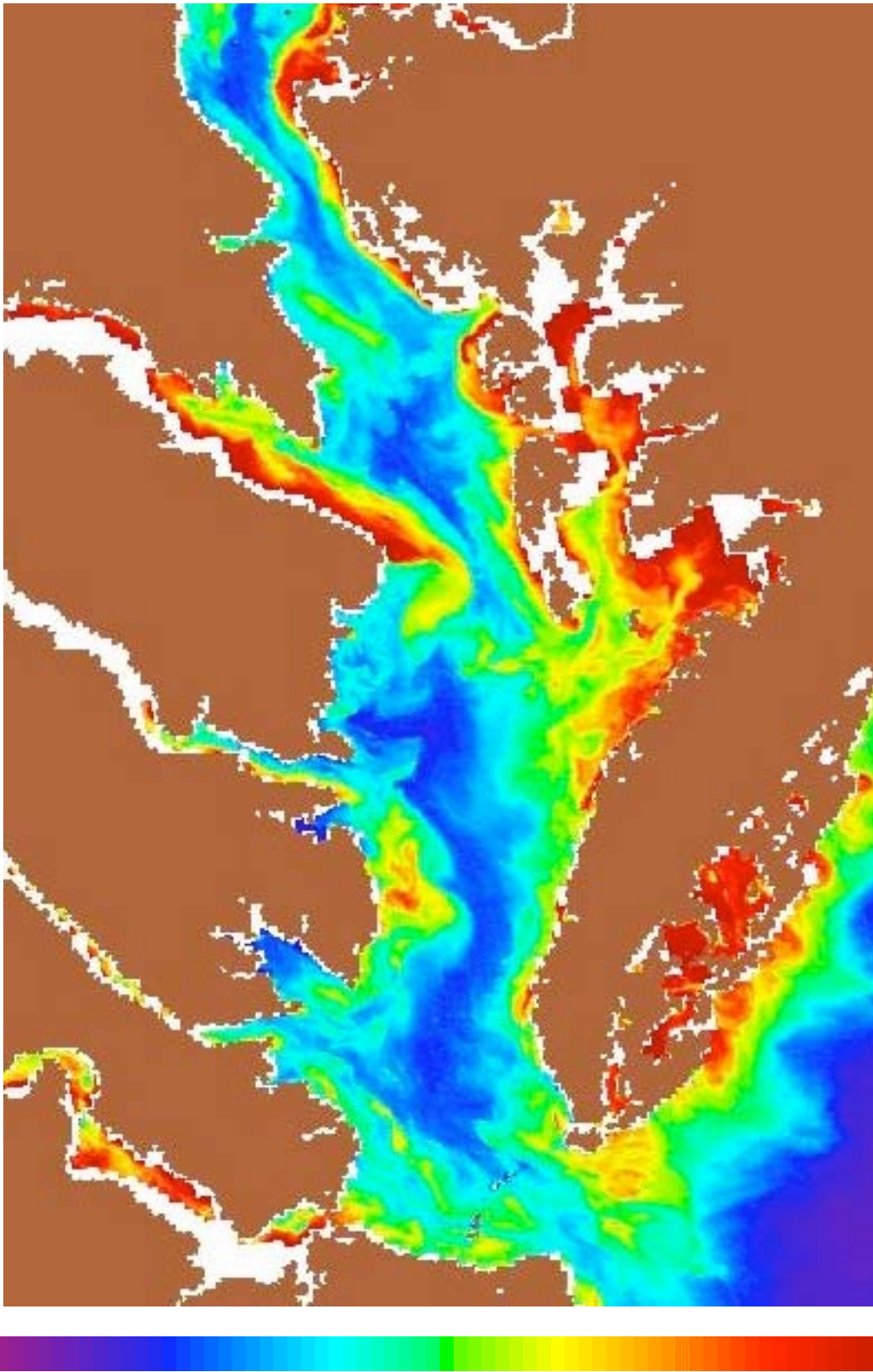


Figure 4: Normalized water-leaving radiance at 645-nm derived from scene of Figure 3. Data was processed at 250-meter resolution and mapped to 255-meter. Scale is -0.1 to $3.0 \text{ mW cm}^{-2} \text{ um}^{-1} \text{ sr}^{-1}$.

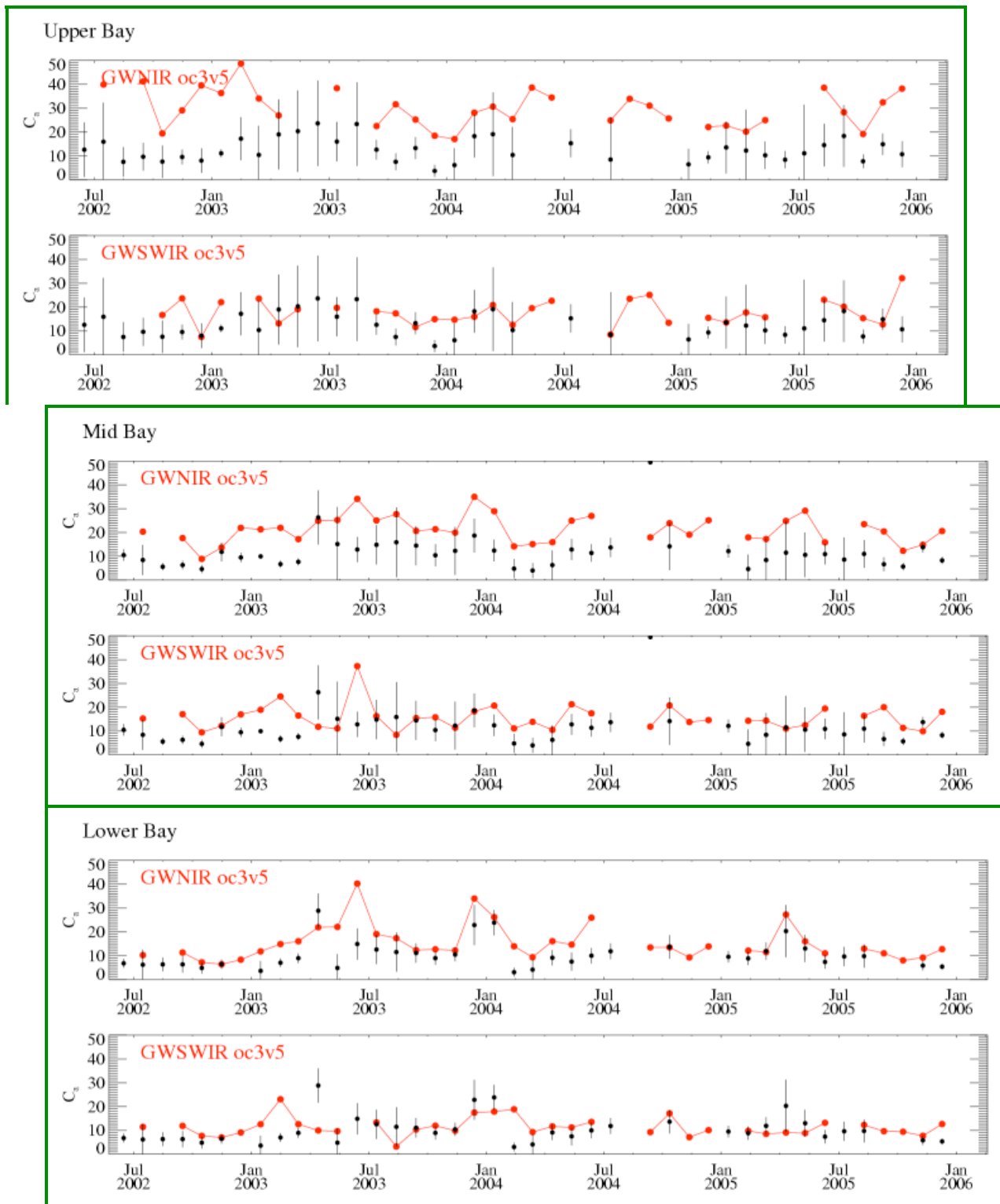


Figure 5: Time-series of monthly mean chlorophyll-a for Chesapeake Bay. Symbols in black show in situ measurements from the Chesapeake Bay Program and Harding with vertical bars to indicate 1 standard deviation. Red symbols and lines show MODIS/Aqua retrievals using the standard atmospheric correction (GWNIR) and the SWIR-based (GWSWIR) for the upper, middle, and lower regions of the Bay. MODIS chlorophyll was derived using the OC3 algorithm. Units are mg m^{-3} .

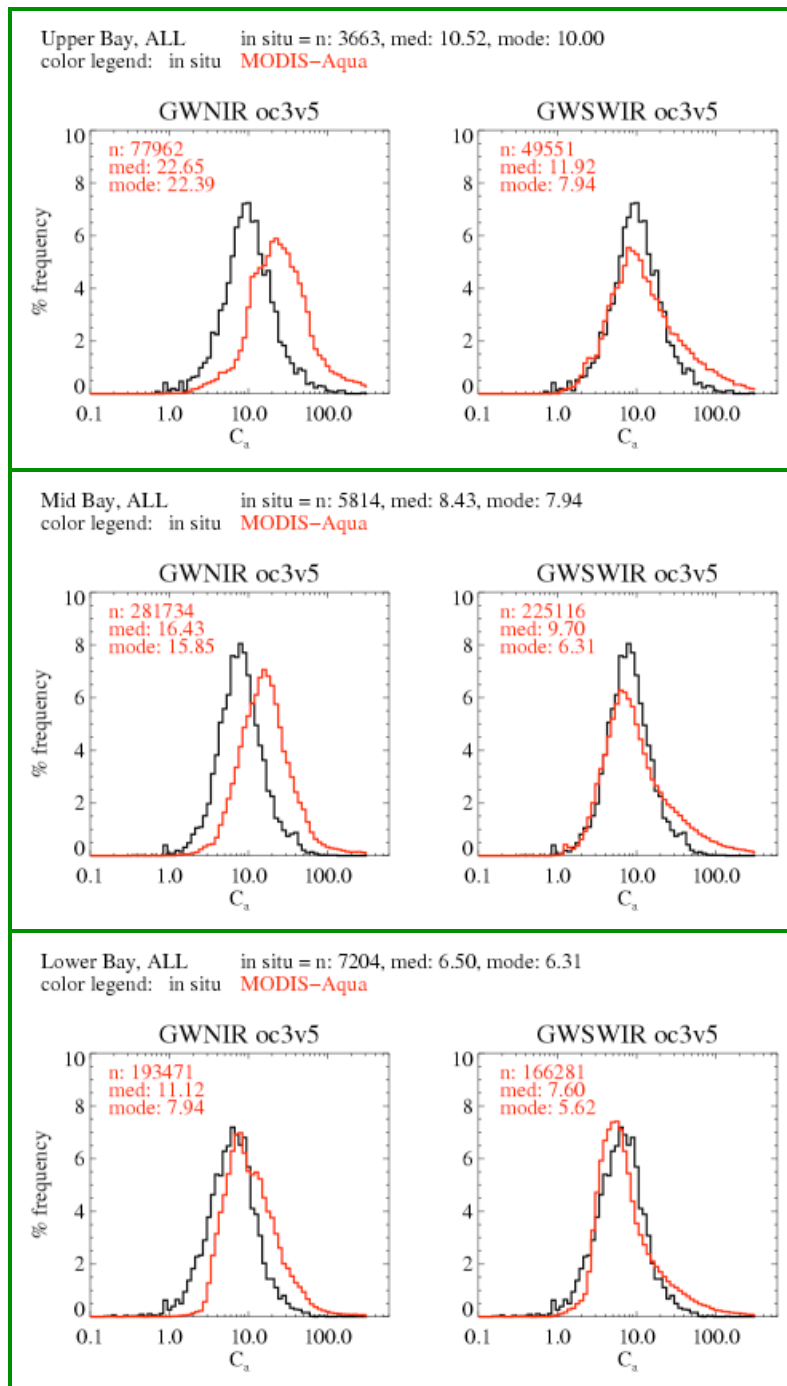


Figure 6: Frequency distributions of chlorophyll-a for Chesapeake Bay. Lines in black show in situ measurements from the Chesapeake Bay Program and Harding, while red lines show MODIS/Aqua retrievals using the standard atmospheric correction (GWNIR) and the SWIR-based correction (GWSWIR) for the upper, middle, and lower regions of the Bay. MODIS chlorophyll was derived using the OC3 algorithm. Units are mg m^{-3}